Research Article: Open Access

VIBGYOR ePress

International Journal of Optics and Photonic Engineering

ISSN: 2631-5092

Tight Focusing Properties of Circularly Polarized Annular Multi-Gaussian Beam through a Uniaxial Birefringent Crystal

R Murugesan[1], D ThiruArul[2], KB Rajesh[2*], M Lavanya[3] and G Mahadevan[4]

[1]Department of Electronics, Erode Arts and Science College, Erode, Tamilnadu, India

[2]Department of Physics, Chikkanna Government Arts College, Tiruppur, Tamilnadu, India

[3]Department of Physics, PSGR Krishnammal College for Women, Coimbatore, India

[4]Department of Mathematics, Gandhigram University, Dindigul, Tamil Nadu, India

Abstract

Focusing properties of circularly polarized annular multi-Gaussian beams through a uniaxial birefringent crystal is investigated numerically by vectorial Debye theory. Results show that the optical intensity in focal region of circularly polarized annular multi-Gaussian beams can be altered considerably by the topological charge [n], beam order [m] and birefringence [Δn]. Many novel focal structures such as focal spot, focal hole and flat top profile of sub wavelength structure are achieved.

Keywords

Uniaxial birefringent crystal, Circularly polarized laser, Annular multi-Gaussian Beam

Introduction

In Recent years, focal shaping of tight-focusing of laser beams such as highly confined focal spot/hole with extended focal depth, multiple focal spots, optical bubble etc., has important applications in high-density optical data storage [1], laser micro/nano-processing [2], particle and electron acceleration [3], super-resolution scanning confocal microscopy [4] and optical trapping [5]. The intensity distribution of the focal structure in the focal region has been frequently discussed [6-13]. To produce different types of intensity distribution in the focal plane one may insert a physical mask in the pupil plane of the objective [14-18]. However, fabricating those physical masks are difficult and their efficiency is also low. On the other hand, optically, uniaxial crystals are performing the same operations without additional devices [19]. Alejo and Deng, et al. studied the properties of light beams propagating in birefringent material [20,21]. The brief explanation of focusing into a birefringent medium is given by Stamnes, Jiang and Dhayalan, et al. [22-26]. A. Ciattoni, et al. analyzed the propagation of radial and azimuthal vortex beam in the uniaxial crystal system [27-29]. Stallinga, et al. briefly explained the vectorial approach of focusing into the uniaxial crystal [30]. Radially and azimuthally polarized vortex beams through a uniaxial crystal system are studied numerically and experimentally [31,32]. Recently properties of circularly polarized beam have explained by many researchers [33-37]. Rao Lian-Zhou, et al. extends the analysis of tightly focusing circularly polarized vortex beams through uniaxial crystals with small axial birefringence [38]. Recently, Murugesan, et al. numerically demonstrated that focal structures such as splitting of single focal spot on to multiple spots and focal shift of maximum intensity in the axial direction can be obtained by tightly focused circularly polarized double ring-shaped beam and axial birefringence [39]. Anthony A. Tovar, et al. introduced a new class of beam called multi-Gaussian beam which consist of a small sum of finite-width Gaussian beams side by side each of which represents an intuitive com-

***Corresponding author:** *KB Rajesh, Department of Physics, Chikkanna Government Arts College, Tiruppur, Tamilnadu, India*

Accepted: October 22, 2018: **Published:** October 24, 2018

Citation: Murugesan R, ThiruArul D, Rajesh KB, Lavanya M, Mahadevan G (2018) Tight Focusing Properties of Circularly Polarized Annular Multi-Gaussian Beam through a Uniaxial Birefringent Crystal. Int J Opt Photonic Eng 3:011

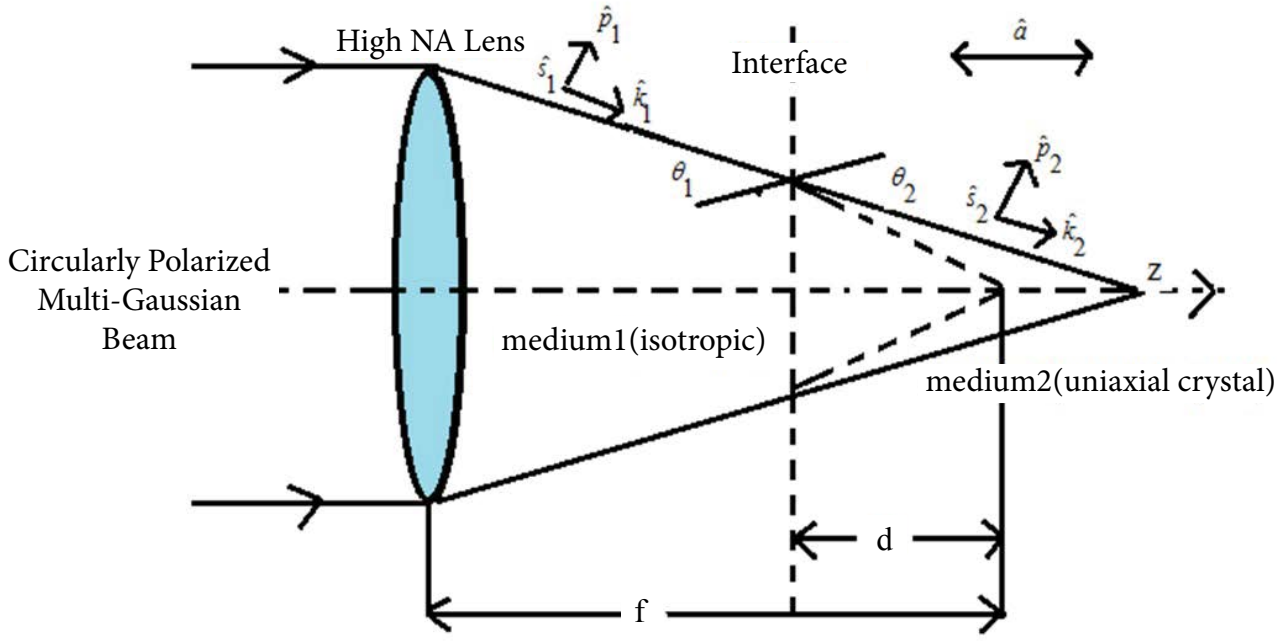

Figure 1: Scheme of the optical system.

ponent of the entire beam. Unlike the flattened Gaussian beams, each of the multi-Gaussian beam components can be traced individually to resort to further series expansion. They proposed multi-Gaussian beam has the advantages of the super-Gaussian while having diffraction characteristics that are analytically solvable [40]. Chen Jian-Nong, et al. proposed annular multi-Gaussian beam mode for sharp focusing [41]. Followed by this, tight focusing properties of annular multigaussian beam are investigated in several works [42-45]. In this paper, we demonstrate the tight focusing properties of circularly polarized annular multi-Gaussian beam through Uniaxial Birefringent Crystal. The intensity distribution of the light beam in focal plane is investigated in detail using numerical simulation.

Theory

The schematic of the focusing system is shown in Figure 1. Here medium 1 is isotropic whereas medium 2 is a Uniaxial birefringent and d is distance between the interface and geometrical focus. Here $\hat{k}_1$ and $\hat{k}_2$ are the wave vectors and $\hat{s}_1$ $\hat{p}_1$ are the polarization vectors in parallel and perpendicular direction to the plane of incidence of medium 1 and $\hat{s}_2$ $\hat{p}_2$ are the corresponding polarization vectors in medium 2. Adopting the theoretical model developed by Stallinga and for the approximation of small axial birefringence of the order of 10^{-3}, the electric field in the focal region is expressed as [30,46].

$$\left\{\begin{array}{l} E_x(r,\psi,z) = \frac{-iE_o}{\pi}\int_0^{\alpha}\int_0^{2\pi} \sin\theta_1\sqrt{\cos\theta_1}P(\theta_1)\exp[ik_2 z\cos\theta_2 + ik_1 r\sin\theta_1\cos(\psi-\phi)] \\ [t_p\cos\theta_2\cos\phi\exp[ik_o(\mathrm{W}+\Delta\mathrm{W})]\pm it_s\sin\phi\exp(iW)]\exp(-\mathrm{i}\phi)d\phi d\theta_1 \end{array}\right\} \quad (1)$$

$$\left\{\begin{array}{l} E_y(r,\psi,z) = \frac{-iE_o}{\pi}\int_0^{\alpha}\int_0^{2\pi} \sin\theta_1\sqrt{\cos\theta_1}P(\theta_1)\exp[ik_2 z\cos\theta_2 + ik_1 r\sin\theta_1\cos(\psi-\phi)] \\ [t_p\cos\theta_2\sin\phi\exp[ik_o(\mathrm{W}+\Delta\mathrm{W})]\pm it_s\cos\phi\exp(iW)]\exp(-\mathrm{i}\phi)d\phi d\theta_1 \end{array}\right\} \quad (2)$$

$$\left\{\begin{array}{l} E_z(r,\psi,z) = \frac{-iE_o}{\pi}\int_0^{\alpha}\int_0^{2\pi} \sin\theta_1\sqrt{\cos\theta_1}P(\theta_1)\exp[ik_2 z\cos\theta_2 + ik_1 r\sin\theta_1\cos(\psi-\phi)] \\ [-t_p\sin\theta_2\exp[ik_o(W+\Delta W)]]\exp(-\mathrm{i}\phi)d\phi d\theta_1 \end{array}\right\} \quad (3)$$

Where r,ψ and z are the cylindrical coordinates and E_o is a constant. $\alpha = \sin^{-1}(NA)$ is the maximal angle determined by the NA of the objective; t_p and t_s are the amplitude transmission coefficients for parallel and perpendicular polarization states respectively, which are given by the Fresnel equations [47].

$$t_s = \frac{2\sin\theta_2\cos\theta_1}{\sin(\theta_1+\theta_2)},\ t_p = \frac{2\sin\theta_2\cos\theta_1}{\sin(\theta_1+\theta_2)\cos(\theta_1-\theta_2)} \quad (4)$$

Here W is the aberration function caused by the mismatch of the refractive indices medium 1 and medium 2, Where ΔW is the phase difference between the ordinary and extraordinary modes in the uniaxial birefringent medium 2. W and ΔW are expressed as [30].

$$W = k_o d(n_2\cos\theta_2 - n_1\cos\theta_1),\ \Delta W = k_o(d+z)\Delta n\sin^2\theta_2/\cos\theta_2 \quad (5)$$

Where $K_o = 2\pi/\lambda$ is the wave numbers in vacuum and $\Delta n = n_e - n_o$ represents the difference between the refractive indices of ordinary and extraordinary modes in the uniaxial crystal. It is assumed that the focusing lens is corrected for aberrations introduced by anisotropic cover layer of thickness d and refractive index $n_2 = n_0$. As a result, $W = 0$. Here $P(\theta_1)$ is the pupil function of the beam; the pupil function of annular multi-Gaussian beams is [41].

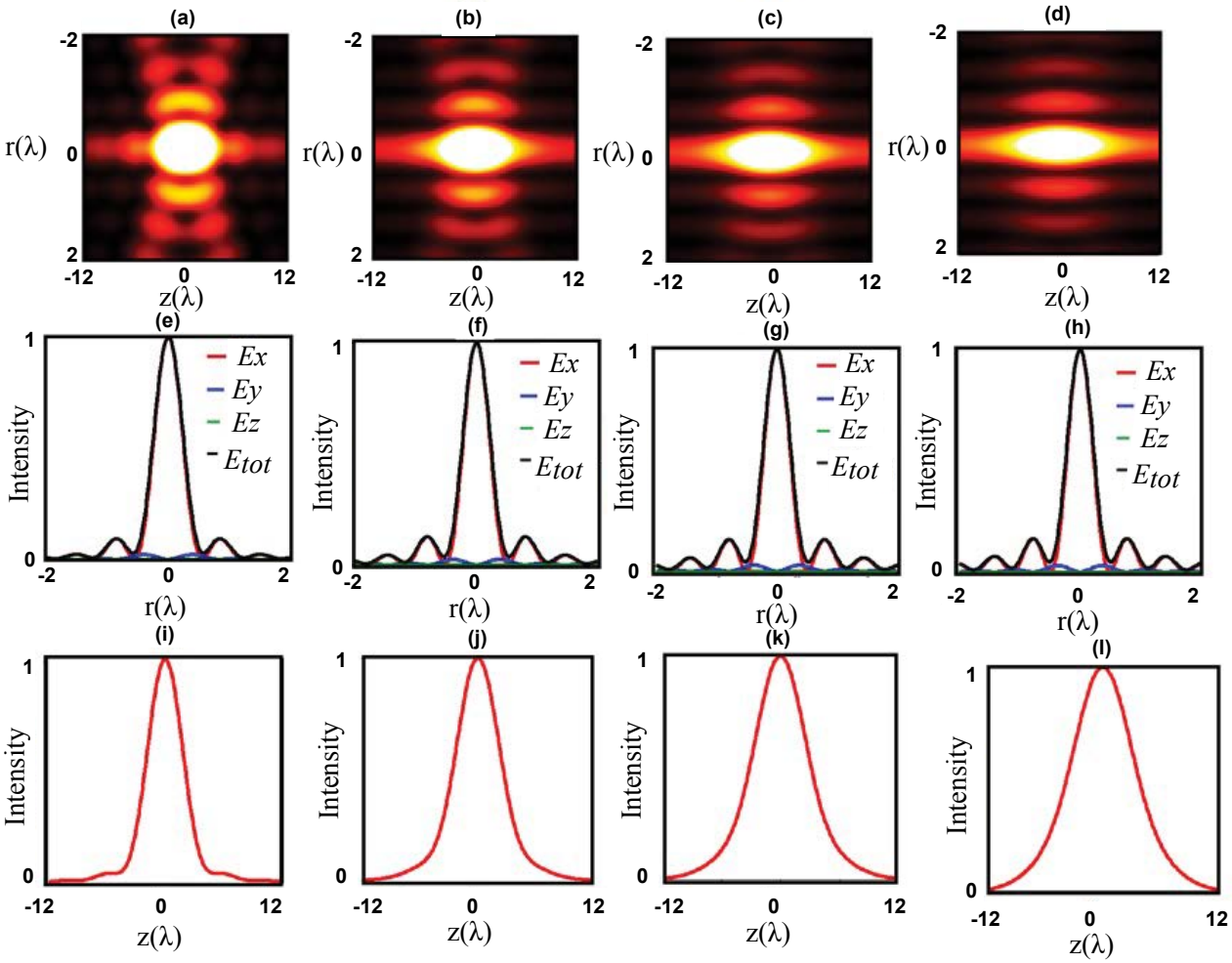

Figure 2: (a-d) are 3D Intensity distribution in the r-z plane corresponding to m = 2,4,6,8 and for Δn = 0; (e-h) are the corresponding 2D intensity measured in the radial axis at the point of maximum on axial intensity; (i-l) are the 2D on axial intensity distribution.

$$P(\theta_1) = \left(\frac{\theta_1}{\theta_o}\right)^m \sum_{n=-N}^{N} \exp\left[-\left(\frac{\theta_1 - \theta_c - n\omega_o}{\omega_o}\right)^2\right] \quad (6)$$

Here, θ_1 is the converging semi-angle. We denote the maximum converging semi-angle as θ_{max} which is related to objective numerical aperture by $\theta_{max} = \arcsin(NA)$. θ_o be an angle which, along with integer m, determines the shape of the modulation function. θ_o is usually choosing to be slightly smaller than θ_{max}. θ_c determine the radial position translation. Here we take $\theta_c = \theta_{max}/2$.

Result and Discussion

The focal properties are evaluated numerically by solving the above equations numerically using the parameters $NA = 0.85$, $n_1 = 1$, $n_2 = 1.5$, $\lambda = 400$ nm, $d = 100$ μm. Figure 2 shows the focal pattern evolved for different beam order (m) of the incident circularly polarized multi-Gaussian beam in the absence of axial birefringence .The Figure 2a, Figure 2b, Figure 2c and Figure 2d shows the 3D intensity in the r-z plane corresponding to m = 2,4,6 and 8 respectively. Figure 2e, Figure 2f, Figure 2g, and Figure 2h shows the respective 2D intensity measured in the radial axis corresponding to the position of maximum on axial intensity. Figure 2i, Figure 2j, Figure 2k and Figure 2l shows the 2D axial intensity distribution. It is noted from the Figure, that increasing the beam orders m increases the focal depth and reduced the FWHM of the generated focal spot.

Table 1: Showing the FWHM and depth of focus achieved for different beam order m and for Δn = 0.

m	Spot size (λ)	Depth of focus (λ)
2	0.53	4.25
4	0.53	5.53
6	0.49	7.07
8	0.48	8.87

Table 1 shows the FWHM and focal depth of the generated focal spot corresponding to different m. It is noted that the E_x component having central maximum dominates the entire focal spot on all the m values. The E_y and E_z components having central minimum is found to be feeble. It is noted that a highly confined focal spot

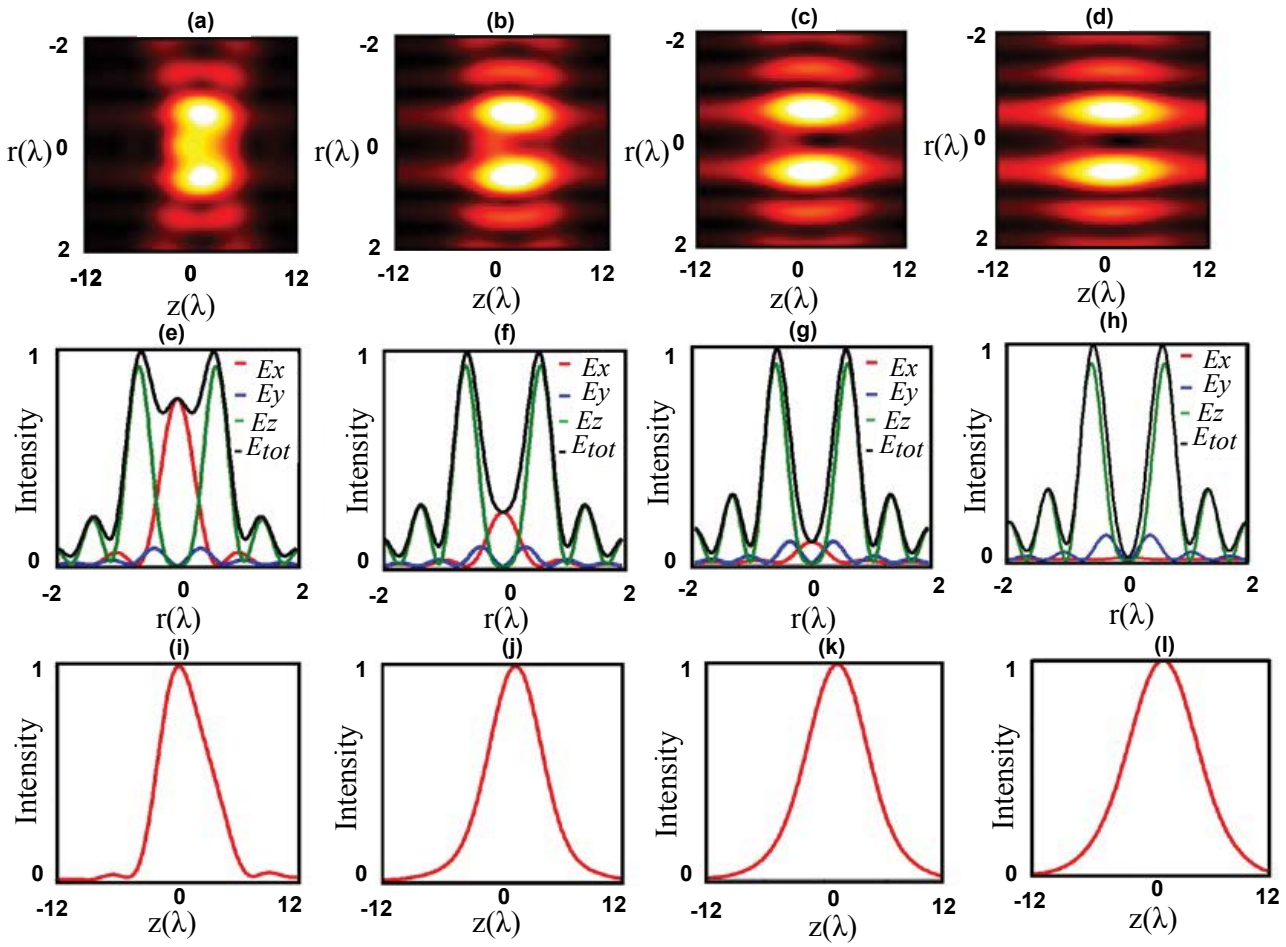

Figure 3: Shows same as Figure 2 but for m = 2,4,6,8 and $\Delta n = 6\times10^{-3}$.

with FWHM of 0.48λ and extend focal depth of 8.87λ is obtained for m = 8. Here focal depth is considered as FWHM of axial intensity.

Figure 3 shows the same as Figure 2 but for the presence of axial birefringence with $\Delta n = 6\times10^{-3}$. It is noted from Figure 2a, Figure 2e and Figure 2i when m = 2,the presence of axial birefringence makes the E_z component having central minimum dominates the focal structure and the resultant focal structure appears to be an radial extended focal spot with large FWHM around 1.8λ with focal depth around 7.16λ. However it is noted from Figure 3b, Figure 3c and Figure 3d and their respective intensity in the radial and axial direction ,that further increasing of beam order to 4,6 and 8 makes the E_z component more dominating than the E_x component having central maximum and the generated focal structure has a central minimum. It is noted from Figure 2b the existence of residual intensity at the centre due to the presence of E_x component is completely vanished and resulted in formation of focal hole as shown in Figure 3d. The on axial intensity calculated at r = 0.58λ shows the depth of focus on the generated focal hole is around 8.46λ and FWHM of focal hole is around 0.65λ. such a dark channel of sub wavelength size and axially extended focal depth finds application in trapping absorbing particles, cold atoms [48] and in high resolution STED microscopy [49].

Hence by properly choosing axial birefringence and beam order of multi-Gaussian beam one can tune a focal structure from a focal spot to a focal hole. We also noted that the on axial intensity is found to be maximum at z = 1.21λ for all the beam order considered. Thus, the presence of axial birefringence generates focal shift effect apart from tuning the focal patterns.

Figure 4 Shows same as Figure 3 but for m = 2,4,6,8 and $\Delta n = 8\times10^{-3}$. It is noted from Figure 4a, Figure 4e and Figure 4i that when m = 2, the generated focal structure is an optical bubble having radial extend of 0.74λ and axial size of 3.05λ. such an optical bubble is useful in trapping and manipulating of particles having refractive index lower than the ambient [50]. Thus, using a single focusing unit, one can tune the focal structure from a focal spot to focal hole and then to an optical bubble. such a tunability in focal structure ensure the capability of trapping particles of refractive index higher or lower than the ambient with single focusing unit. Hence one

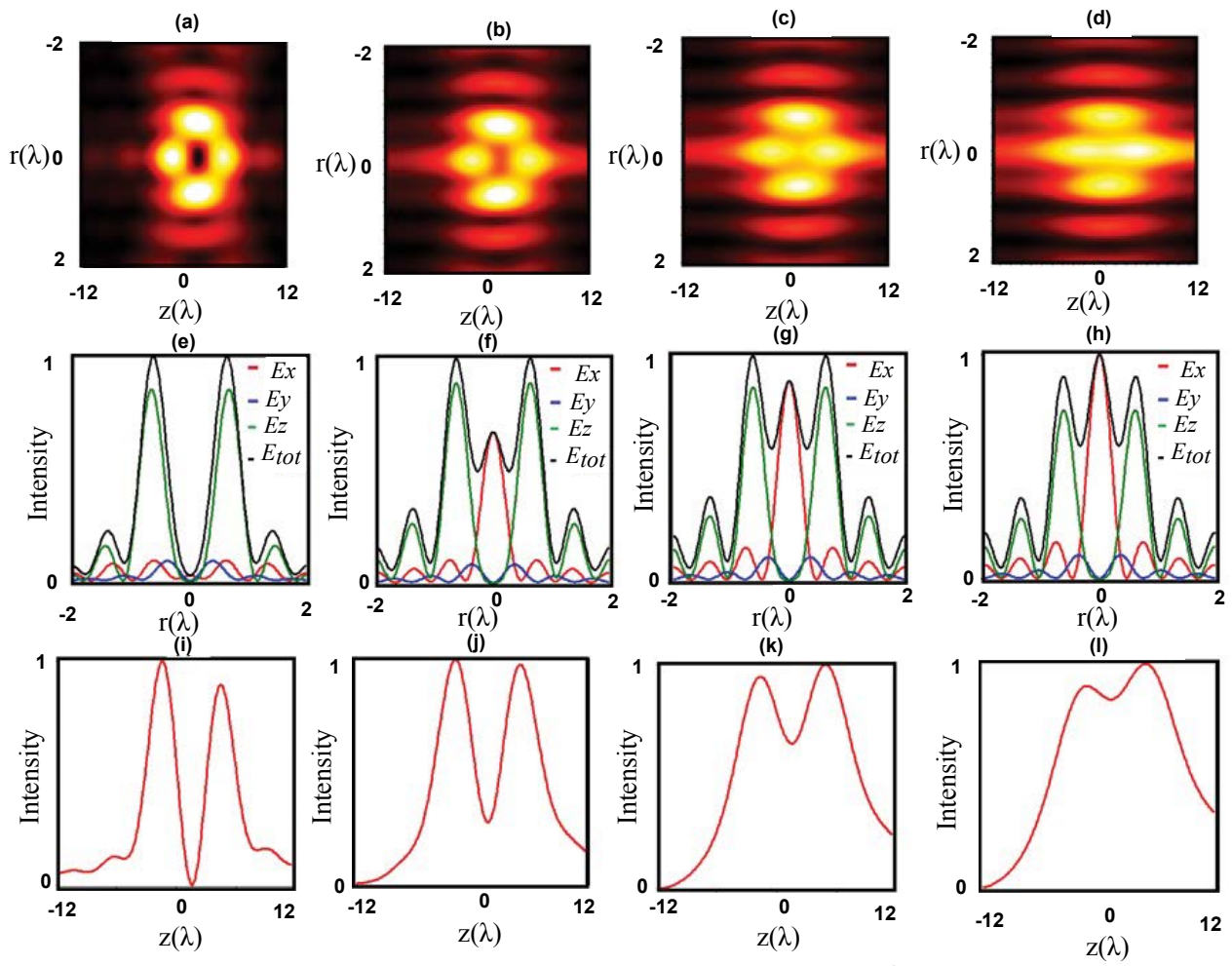

Figure 4: Shows same as Figure 3 but for m = 2,4,6,8 and $\Delta n = 8 \times 10^{-3}$.

can avoid the problem of mounting and aligning specially designed dedicated binary phase/amplitude filters to modulate the focal patterns. It is noted that the centre of the bubble is located at z = 1.64λ. Figure 4b, Figure 4c and Figure 4d shows that further increasing of *m* makes the E_x component dominating and created a non-zero central focal pattern.

Figure 5 shows the same as Figure 4 but for $\Delta n = 10 \times 10^{-3}$. It is noted from the Figure 5a, when *m* = 2, the generated focal structure is found to be axially shifted and splitted focal spots with a residual intensity between them. It is noted from Figure 5e that the E_x component starts dominating the focal structure. We also noted that further increasing *m* to 4, 6 and 8 results in further increasing of E_x component which results in a highly confined focal spot with FWHM around 0.48λ. However, it is noted from the on axial intensity plots shown in Figure 5j, Figure 5k and Figure 5l that the on axial bumpy structure turns to be flattop and axially extended corresponding to the beam order *m* = 6. Such a flat top focus is useful in applications such as improved printing filling factor, improved uniformity and quality in material processing, microlithography, medical treatment [51-53].

Table 2: Showing the FWHM and depth of focus achieved for different beam order m and for Δn = 10 × 10^{-3}.

m	Spot size (λ)	Depth of focus (λ)	Shift Z (λ)
2	0.57	5.12	0.88
4	0.52	15.09	1.84
6	0.49	16.48	1.91
8	0.48	18.05	2.20

The depth of focus and spot size of the generated focal spots is shown in Table 2. It is noted that a smallest focal spot size around 0.48λ with maximum focal depth of 18.05λ and focal shift of 2.20λ is noted for *m* = 8. Such a focal spot of sub wavelength size and extended focal depth is highly useful in applications such as high-density optical data storage, particle acceleration, biomedical imaging and in optical trapping [1,54-56]. Thus, by modulating beam order of a circularly polarized annular multi Gaussian beam and axial birefringence of a uniaxial crystal one can generate many novel focal structures usable for nano scale applications such as high-density optical recording, particle trapping and material processing etc.

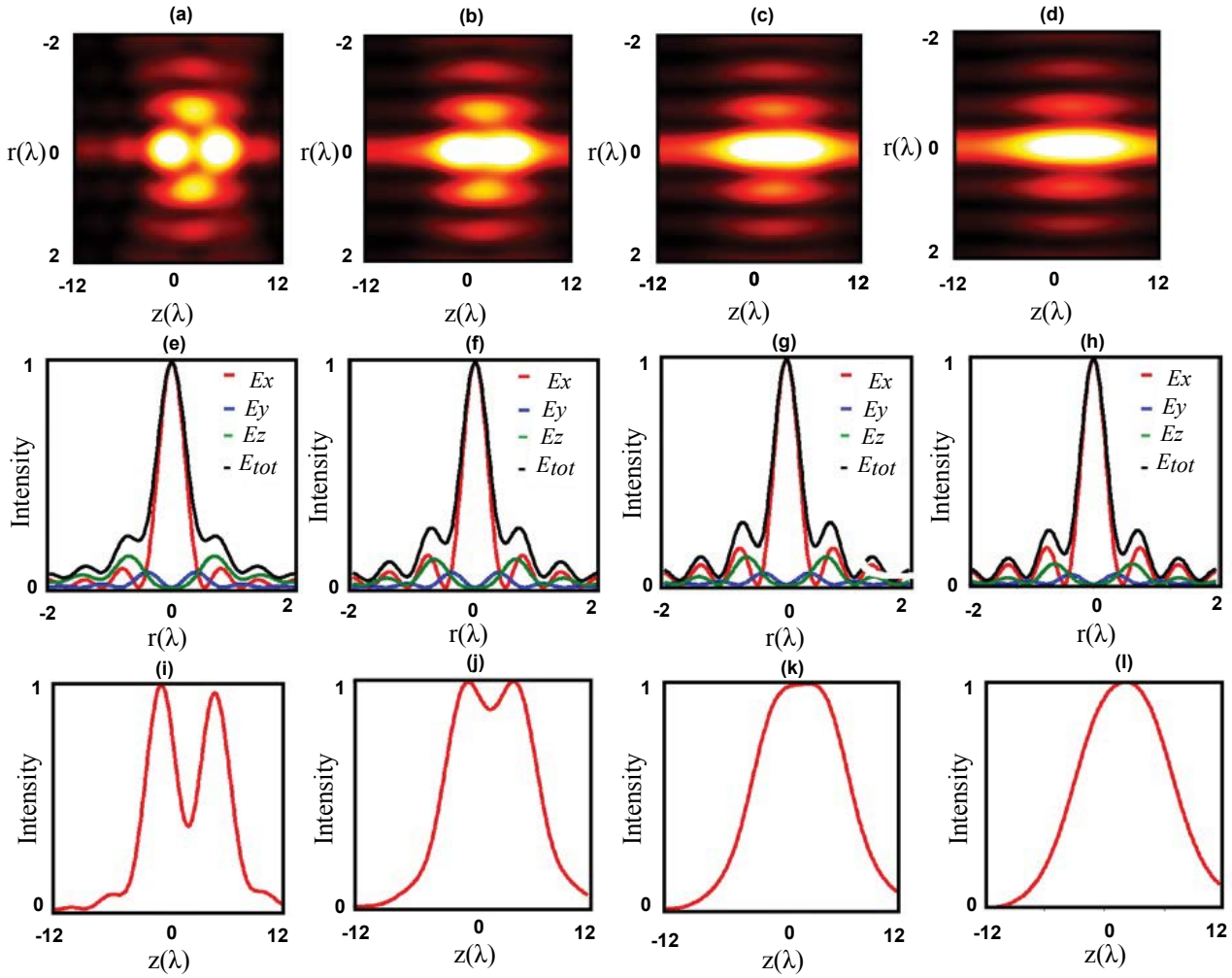

Figure 5: Shows same as Figure 4 but for m = 2,4,6,8 and $\Delta n = 10 \times 10^{-3}$.

Conclusion

In conclusion, a simple method to achieve tunability of focal structures suitable for nanoscale applications using the effect of axial briefinges on tightly focused circularly polarized annular multigaussian beams is demonstrated numerically using vector diffraction theory. It is observed that many novel focal patterns such as focal spot/hole of extended focal depth, optical bubble and flat top profile of sub wavelength scale is achieved by properly modulating the axial birefringence and order of multi Gaussian beam. The authors expect such a study is useful in applications such as optical trapping, high density optical recording and in optical material processing etc.

References

1. Zhang Y, Bai J (2009) Improving the recording ability of a near-field optical storage system by higher-order radially polarized beams. Opt Express 17: 3698-3706.
2. Lou K, Qian SX, Wang XL, Li Y, Gu B, et al. (2012) Two-dimensional microstructures induced by femto second vector light fields on silicon. Opt Express 20: 120-127.
3. Fortin PL, Piche M, Varin C (2010) Direct-field electron acceleration with ultrafast radially polarized laser beams: Scaling laws and optimization. J Phys B: At Mol Opt Phys 43: 025401.
4. Kozawa Y, Hibi T, Sato A, Horanai H, Kurihara M, et al. (2011) Lateral resolution enhancement of laser scanning microscopy by a higher-order radially polarized mode beam. Opt Express 19: 15947-15954.
5. Zhang Y, Suyam T, Ding B (2010) Longer axial trap distance and larger radial trap stiffness using a double-ring radially polarized beam. Opt Lett 35: 1281-1283.
6. Chen Z, Zhao D (2012) 4Pi focusing of spatially modulated radially polarized vortex beams. Opt Lett 37: 1286-1288.
7. Wang H, Shi L, Lukyanchuk B, Sheppard C, Chong CT (2008) Creation of a needle of longitudinally polarized light in vacuum using binary optics. Nature Photonics 2: 501-505.
8. Wang J, Chen W, Zhan Q (2012) Creation of uniform three-dimensional optical chain through tight focusing of space-variant polarized beams. J Opt 14: 055004.
9. Youngworth KS, Brown TG (2000) Focusing of high numerical aperture cylindrical vector beams. Opt Express 7: 77-87.
10. Helseth LE (2001) Roles of polarization, phase and amplitude in solid immersion lens system. Opt Commun 191: 161-172.

Citation: Murugesan R, ThiruArul D, Rajesh KB, Lavanya M, Mahadevan G (2018) Tight Focusing Properties of Circularly Polarized Annular Multi-Gaussian Beam through a Uniaxial Birefringent Crystal. Int J Opt Photonic Eng 3:011

11. Weichao Yan, Zhongquan Nie, Xueru Zhang, Yuxiao Wang, Yinglin Song (2017) Theoretical guideline for generation of an ultralong magnetization needle and a super-long conveyed spherical magnetization chain. Opt Express 25: 22268-22279.

12. Andres Aragoneses, Nurul TI, Michael E, Arturo L, Jungsang K, et al. (2018) Bounding the outcome of a two-photon interference measurement using weak coherent states. Opt Lett 43: 3806-3809.

13. Weichao Yan, Zhongquan Nie, Xiaofei Liu, Guoqiang Lan, Xueru Zhang, et al. (2018) Dynamic control of transverse magnetization spot arrays. Opt Express 26: 16824-16835.

14. Liang J, Kohn Jr RN, Becker MF, Heinzen DJ (2009) 1.5% root-mean-square flat-intensity laser beam formed using a binary-amplitude spatial light modulator. Appl Opt 48: 1955-1962.

15. Wu G, Wang F, Cai Y (2014) Generation and self-healing of a radially polarized Bessel-Gauss beam. Phys Rev A 89: 043807.

16. Suresh P, Gokulakrishnan K, Mariyal C, Rajesh KB, Sivasubramonia Pillai TV (2013) Effect of binary phase plate on incident radially polarized hollow Gaussian beam. Optik 124: 5350-5352.

17. Zhan Q (2009) Cylindrical vector beams: From mathematical concepts to applications. Advances in Optics and Photonics 1: 1-57.

18. Li J, Gao X, Zhuang S, Huang C (2010) Focal shift and focusing properties generation by radial cosine phase masks. Optik 121: 821-825.

19. Wang S, Xie X, Gu M, Zhou J (2015) Optical sharper focusing in an anisotropic crystal. J Opt Soc Am A Opt Image Sci Vis 32: 1026-1031.

20. Alejo MA, Aguilar MR (2006) Optical path difference in a plane-parallel uniaxial plate. J Opt Soc Am A Opt Image Sci Vis 23: 926-932.

21. Deng D, Yu H, Xu S, Shao J, Fan Z (2008) Propagation and polarization properties of hollow Gaussian beams in uniaxial crystals. Optics Communications 281: 202-209.

22. Stamnes JJ, Jiang D (1998) Focusing of electromagnetic waves into a uniaxial crystal. Optics Communications 150: 251-262.

23. Jiang D, Stamnes JJ (1999) Numerical and asymptotic results for focusing of two-dimensional waves in uniaxial crystals. Optics Communications 163: 55-71.

24. Jiang D, Stamnes JJ (2000) Numerical and experimental results for focusing of Two-dimensional electromagnetic waves into uniaxial crystals. Optics Communications 174: 321-334.

25. Stamnes JJ, Dhayalan V (2001) Transmission of a two-dimensional Gaussian beam into a uniaxial crystal. J Opt Soc Am A Opt Image Sci Vis 18: 1662-1669.

26. Jain M, Lotsberg JK, Stamnes JJ, Frette O, Velauthapillai D, et al. (2009) Numerical and experimental results for focusing of three-dimensional electromagnetic waves into uniaxial crystals. J Opt Soc Am A Opt Image Sci Vis 26: 691-698.

27. Ciattoni A, Crosignani B, Porto PD (2001) Vectorial theory of propagation in uniaxially anisotropic media. J Opt Soc Am A Opt Image Sci Vis 18: 1656-1661.

28. Ciattoni A, Cincotti G, Palma C (2002) Propagation of cylindrically symmetric fields in uniaxial crystals. J Opt Soc Am A Opt Image Sci Vis 19: 792-796.

29. Cincotti G, Ciattoni A, Sapia C (2003) Radially and azimuthally polarized vortices in uniaxial crystals. Optics Communications 220: 33-40.

30. Stallinga S (2001) Axial birefringence in high-numerical-aperture optical systems and the light distribution close to focus. J Opt Soc Am A Opt Image Sci Vis 18: 2846-2859.

31. Zhang Z, Pu J, Wang X (2008) Tight focusing of radially and azimuthally Polarized vortex beams through a uniaxial birefringent crystal. Appl Opt 47: 1963-1967.

32. Yonezawa K, Kozawa Y, Sato S (2008) Focusing of radially and azimuthally polarized beams through a uniaxial crystal. J Opt Soc Am A Opt Image Sci Vis 25: 469-472.

33. Zhan Q (2006) Properties of circularly polarized vortex beams. Opt Lett 31: 867-869.

34. Zhang Y, Bai J (2008) High-density all-optical magnetic recording using a high-NA lens illuminated by circularly polarized pulse lights. Physics Letters A 372: 6294-6297.

35. Zhang Y, Bai J (2009) Theoretical study on all-optical magnetic recording using a solid immersion lens. Journal of the Optical Society of America B 26: 176-182.

36. Zhang Y, Okuno Y, Xub X (2010) Symmetry properties of three-dimensional magnetization distributions induced by focused circularly polarized lights. Optik - International Journal for Light and Electron Optics 121: 2062-2066.

37. Zhang Z, Fan H, Xu HF, Qu J, Huang W (2015) Three-dimensional focus shaping of partially coherent circularly polarized vortex beams using a binary optic. J Opt 17: 065611.

38. Rao LZ, Wang ZC, Zheng XX (2008) Tightly focusing of circularly polarized vortex beams through a uniaxial birefringent crystal. Chinese Phys Lett 25: 3223-3226.

39. Murugesan R, Pasupathy N, ThiruArul D, Rajesh KB, Velauthapillai Dhayalan (2017) Generating multiple focal structures with circularly polarized double ring-shaped beam and axial birefringence. J Opt 46: 403.

40. Tovar AA (2001) Propagation of flat-topped multi-Gaussian laser beams. J Opt Soc Am A 18: 1897-1904.

41. Nong CJ, Feng XQ, Gang W (2011) Tight focus of a radially polarized and amplitude modulated annular multi-Gaussian beam. Chinese Phys B 20: 114211.

42. Chandrasekaran R, Prabakaran K, Rajesh KB, Mohamed Musthafa A, Ravi V (2016) Tight focusing properties of cylindrically polarized annular multi-Gaussian beam. Optik - International Journal for Light and Electron Optics 127: 7537-7542.

43. CM Sundaram (2016) Creation of super long transversely polarized optical needle using azimuthally polarized multi Gaussian beam. Chinese Phys Lett 33: 064203.

44. Prabakaran K, Rajesh KB, Hariharan V, Aroulmoji V, Anbarasan PM, et al. (2016) Creation of sub wavelength focal spot segment using longitudinally polarized multi Gaussian beam. Int J Adv Sci Eng 2: 164-167.

45. Charles JW, Prabakaran K, Rajesh KB (2014) Generation of sub wavelength super long dark channel using azimuthally polarized annular multi-Gaussian beam. Optical and Quantum Electronics 46: 1079-1086.

Citation: Murugesan R, ThiruArul D, Rajesh KB, Lavanya M, Mahadevan G (2018) Tight Focusing Properties of Circularly Polarized Annular Multi-Gaussian Beam through a Uniaxial Birefringent Crystal. Int J Opt Photonic Eng 3:011

46. Gu M (2000) Advanced optical imaging theory. Springer, Berlin, New York.

47. Born M, Wolf E (1999) Principles of optics. (7th edn), Cambridge University Press, Cambridge, United Kingdom.

48. Xu P, He XD, Wang J, Zhan MS (2010) Trapping a single atom in a blue detuned optical bottle beam trap. Opt Lett 35: 2164-2166.

49. Willig KI, Rizzoli SO, Westphal V, Jahn R, Hell SW (2006) Sted microscopy reveals that synaptotagmin remains clustered after synaptic vesicle exocytosis. Nature 440: 935-939.

50. Zhao Y, Zhan Q, Li YP (2004) Design of DOE for the control of optical “bubble” generated by highly focused radially polarized beam. Proceedings of the SPIE 5514: 616-625.

51. Dickey FM, Holswade SC (2000) Laser beam shaping: Theory and techniques. Marcel Dekker, New York, USA.

52. Romero LA, Dickey FM (1996) Lossless laser beam shaping. Journal of the Optical Society of America A 13: 751-760.

53. Homburg O, Mitra T (2012) Gaussian-to-top-hat beam shaping: An overview of parameters, methods, and applications. Proc SPIE 8236.

54. Varin C, Piche M, Porras MA (2005) Acceleration of electrons from rest to GeV energies by ultra-short transverse magnetic laser pulses in free space. Phys Rev E Stat Nonlin Soft Matter Phys 71: 026603.

55. Dehez H, Piche M, De Koninck Y (2009) Enhanced resolution in two-photon imaging using a TM01 laser beam at a dielectric interface. Opt Lett 34: 3601-3603.

56. Zhan Q (2004) Trapping metallic Rayleigh particles with radial polarization. Opt Express 12: 3377-3382.

Citation: Murugesan R, ThiruArul D, Rajesh KB, Lavanya M, Mahadevan G (2018) Tight Focusing Properties of Circularly Polarized Annular Multi-Gaussian Beam through a Uniaxial Birefringent Crystal. Int J Opt Photonic Eng 3:011